Photo-Induced Inverse Vulcanization

Jinhong Jia,[1§] Jingjiang Liu,[1§] Zhi-Qiang Wang,[2] Tao Liu,[3] Peiyao Yan,[4] Xueqing Gong,[2*] Chengxi Zhao,[2,3] Linjiang Chen,[2,3,5] Congcong Miao,[1] Wei Zhao,[3] Shanshan (Diana) Cai,[4] Xi-Cun Wang,[1] Andrew I. Cooper,[2,3*] Xiaofeng Wu,[1,2,3*] Tom Hasell,[1,4*] Zheng-Jun Quan[1*]

[1] College of Chemistry and Chemical Engineering, Gansu International Scientific and Technological Cooperation Base of Water-Retention Chemical Functional Materials, Northwest Normal University, Lanzhou 730070, P.R. China
[2] Key laboratory for Advanced Materials and Joint International Research Laboratory of Precision Chemistry and Molecular Engineering, Feringa Nobel Prize Scientist Research Centre, School of Chemistry and Molecular Engineering, East China University of Science and Technology, Shanghai, 200237, P. R. China
[3] Leverhulme Research Centre for Functional Materials Design, Materials Innovation Factory, and Department of Chemistry, University of Liverpool, Liverpool, UK L69 7ZD
[4] Department of Chemistry, University of Liverpool, Liverpool, UK L69 7ZD
[5] School of Chemistry, University of Birmingham, Edgbaston, Birmingham, UK B15 2TT

Corresponding Emails: aicooper@liverpool.ac.uk; xgong@ecust.edu.cn; xfwu@liverpool.ac.uk; T.Hasell@liverpool.ac.uk；quanzhengjun@hotmail.com；

[§]: These authors contribute equally to this work.

The inverse vulcanization (IV) of elemental sulfur to generate sulfur-rich functional polymers has attracted much recent attention. However, the harsh reaction conditions required, even with metal catalysts, constrains the range of feasible crosslinkers. We report here a photo-induced IV that enables reaction at ambient temperatures, greatly broadening the scope for both substrates and products. These conditions enable volatile and gaseous alkenes and alkynes to be used in IV, leading to sustainable alternatives for environmentally harmful plastics that were hitherto inaccessible. Density functional theory calculations reveal significantly different energy barriers for thermal, catalytic, and photoinduced IV processes. This protocol circumvents the long curing times that are common in IV, generates no H_2S by-products, and produces high molecular weight polymers (up to 460,000 $gmol^{-1}$) with almost 100 % atom economy. This photo-induced IV strategy advances both the fundamental chemistry of IV and its potential industrial application to generate materials from waste feedstocks.

Elemental sulfur (S_8), a byproduct of the petrochemical-industry removed from crude oil and natural gas during refining, is cheap, abundant, and underutilized.[1-3] Seventy million tons of S_8 are produced annually with very little consumption, which leads to megaton quantities of S_8 being stockpiled in the open-air for decades, incurring unexplored environmental costs.[4-5] The

emergence of organic polymers synthesized from S_8 *via* the inverse vulcanization (IV) reaction has therefore provoked much recent interest.[1,4-8] This stems from the new chemistry and new classes of organic polymers, coupled with the potential to reduce the environmental concerns associated with our heavy and unsustainable reliance on plastics derived from petroleum feedstocks. Since the pioneering work of Pyun and coworkers in 2013,[9] significant advances have been made in both the IV process itself and in various applications that are based on the unique properties of these polymers (Figure 1). In particular, the range of available organic crosslinkers has been expanded by Pyun,[10-14] Chalker,[15-17] Hasell,[18-21] Theato,[22-25] Mecerreyes,[26-28] and Smith[29-32] and coworkers. Conventional petrochemical derived crosslinkers for IV include 1,3-diisopropenylbenzene,[9] divinylbenzene,[26,33-34] 1,3,5-triisopropenylbenzene,[35] 1,4-diphenylbutadiyne,[11] styrene,[12] vinyl aniline,[36] vinylbenzene chloride,[37] bismaleimide,[34] and cycloalkenes.[38] Inspired by the initial "green" nature of the IV reaction, this range of crosslinkers has also been broadened beyond to encompass more renewable and naturally abundant crosslinkers such as terpenes and mono-, tri-, and cyclic-terpene analogues,[15,20,39-41] vegetable oils[16,19,22,42,43], industrial byproducts--dicyclopentadiene (DCPD),[20] and other unsaturated compounds.[23,29,34,44-45]
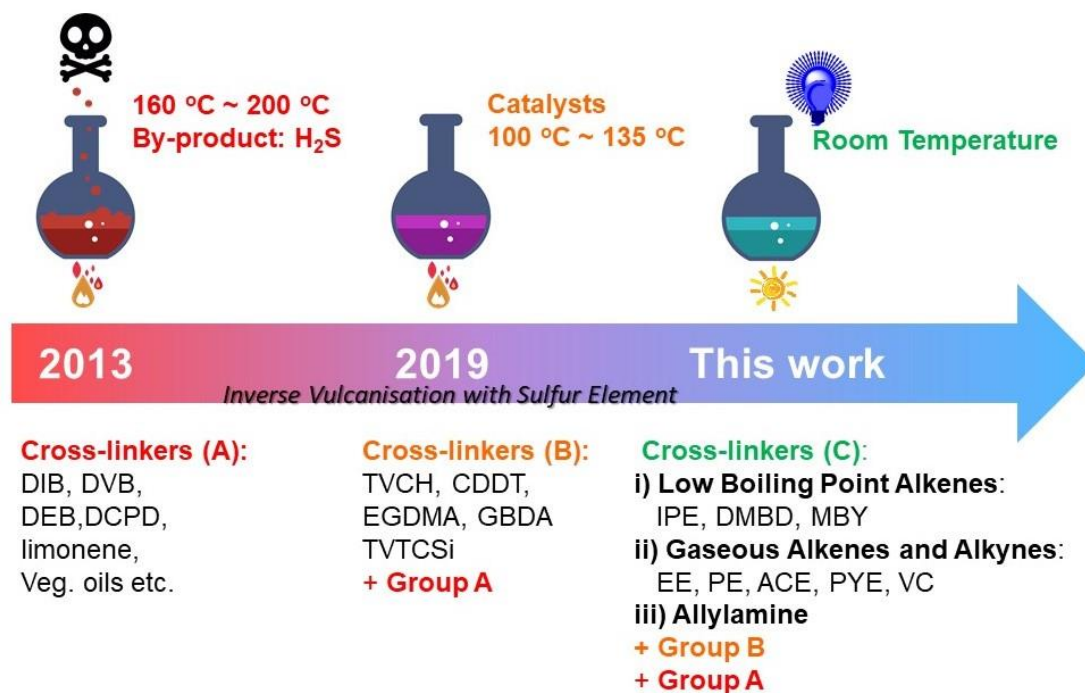
Figure 1. Key milestones in the development of inverse vulcanization (IV) of elemental sulfur.

However, there are still significant challenges for IV, such as developing methods that allow copolymerization of organic monomers with S_8 at lower temperatures (Figure 1).[5] The ring opening of S_8 to generate active sulfur species, typically either free sulfur radicals or anionic sulfur, requires temperature of 160 °C or higher. As well as being energy intensive, this leads to inconsistent polymer properties, toxic H_2S gas production, and uncontrollable auto-acceleration.[4-5] To tackle this, the optimization of the IV reaction conditions has been explored,[18,45-48] and the recent introduction of metal catalysts into IV reactions has significantly advanced the fundamental chemistry, expanding the range of viable crosslinkers.[18] By using 1 wt.% of a metal diethyldithiocarbamates (DTC) catalyst, the reaction temperature can be lowered from 160-200 °C to around 100-135 °C through an alternative catalytic pathway.[5,18] This inhibits the generation of toxic H_2S gas as a byproduct. The use of prepolymers to lower reaction temperatures to a similar range has been reported by the Pyun[46] and Jenkins[47] groups, respectively. It was also demonstrated that 4-vinlyaniline and *N*-methylimidazole can

accelerate the IV reaction via different mechanisms.[36,45] Recently, a room temperature conversion from elemental sulfur to functional polythioureas was reported for a specific case through a catalyst-free multicomponent polymerization of sulfur, aliphatic diamines, and diisocyanides, which though may not be classified as common IV.[49]

Notwithstanding these advances, a reaction temperature of 100-135 °C is still too high to permit the use of many desirable crosslinkers—for example, because they are either volatile or thermally sensitive—and the recently reported room temperature route has not been shown to be generalizable.[49] Here we report a photo-induced IV reaction between elemental sulfur and alkene- and alkyne-crosslinkers at ambient temperatures to afford S-rich polymers (Figure 1C, Extended Data Figure 1b, c). These photo-induced IV polymerizations were carried out catalyst-free at room temperature (18-20 °C), without any extended curing step. There was no toxic H_2S by-product, and the process circumvents auto acceleration of the polymerization reaction. Most significantly, the low reaction temperature allows low-boiling point alkenes and alkynes crosslinkers such as ethylene, propene, acetylene, propyne, and vinyl chloride-many of which are inexpensive industrial gases to be used in IV polymerization. The molecular weights (M_w) of obtained polymers could reach 460,000 $gmol^{-1}$ with polydispersity index (PDI) of 1-1.5 for the soluble polymer fraction. This process significantly enhances the prospects for the commercial application of IV chemistry by allowing room temperature reactions and a greatly broadened selection of crosslinkers and co-monomers.

Results and Discussion

Investigation of photo sources for IV reaction. We conducted the reaction of diisopropenylbenzene (DIB) with S_8 as a model reaction. Successful photo-induced IV was achieved with light of a specific wavelength (380 and 435 nm, 10 W) at ambient temperature

with and without co-catalyst. No reaction was observed in the absence of light with the correct wavelength (Entries 1-4, Table S2). A golden-orange to orange-red color solid was obtained for the model reaction with 380 nm wavelength of UV light for 48 h at room temperature with/without $Zn(DTC)_2$ co-catalyst (1 wt%). ^{1}H NMR spectroscopy indicates clean conversion to one product identified as poly(S-DIB) (Figures S5b, S8). The same reaction with 435 nm UV light (6 h) afforded black solid products. ^{1}H NMR, FTIR, PXRD, TGA, and DSC results confirm conversion to S-rich polymers (Figures 2c-f, S5). No reaction occurred at all even after 72 h for the same reaction with 520 nm or higher wavelength UV light irradiation. Polymers generated under thermal conditions with and without the $Zn(DTC)_2$ catalyst showed glass transition temperatures (T_g) of 31.7 °C and 29.8 °C respectively. No T_g was observed in the DSC trace for the polymer produced by photo-polymerization. Significantly higher molecular weights (M_w: 240,000 gmol^{-1} under photopolymerization vs 100,000 gmol^{-1} under heating at 160 °C) as well as lower polydispersity indices (PDI: 1.47 vs 4.18 under heating at 160 °C) were observed for the polymer produced by photopolymerisation. The measured M_w was based on the soluble fraction of the polymers (DMF solvent). There was also a significant insoluble fraction (up to 80 wt.%) of presumably crosslinked material. This was further evidenced by the solubility tested in a series of organic solvents (Figures 2g, S9, Extended Data Fig 3a).

However, there is still a question if the soluble/insoluble fractions have significant difference in composition, rather than simply degree of crosslinking/Mw. To clarify this point, more experiments and characterizations were carried out on the obtained polymers by exposing to chloroform and dividing into soluble and insoluble fractions (Figure S10-S14, Table S3, Extended Data Fig 4). The solid nuclear magnetic resonance spectra (^{13}C NMR) of the insoluble matter and the mixture of obtained polymers were consistent. The bonding mode of the soluble and insoluble fractions as well as the mixture of obtained polymers was analyzed by XPS: the spectra of all three samples were consistent, but there is a difference between the

degree of polymerization, which affects the solubility. TGA comparison shows a lower onset of degradation, and reduced char mass, for the soluble fraction in comparison to the insoluble fraction, which would be consistent with lower molecular weight, a lower degree of crosslinking, and a higher proportion of sulfur, which is also shown by Elemental Analysis (Table S4). High performance liquid chromatography (HPLC) suggests there is still some un-stabilized S_8 present in the products (Figure S14), which is removed into the soluble fraction, consistent with the higher proportion of sulfur detected for that fraction. Powder X-ray diffraction (PXRD, Figures 2d, S5d) confirmed the products were amorphous, and no crystalline S_8 was detected. Thermogravimetric analysis (TGA) explored the thermal stability of poly(S-DIB) under different photochemical and thermal conditions (Figures 2e, S5e). Tests with lead acetate showed H_2S by-products were detected for thermal reactions, but not for the equivalent photo-reaction (Figures S6, S7, Extended Data Fig. 2).

Of note is that the lack of agitation during reaction, and uneven reactor geometry, might lead to inhomogeneity in the products. To examine the homogeneity in the reactions as usually performed, we divided the reaction of the same vessel into three parts from the center to the periphery, and tested the thermal stability separately (Figure S15, Extended Data Fig. 6a-e, 6i). The results show that from the center to the periphery, the thermal stability decreases successively because of uneven mixing and distance from the light source. The different light density leads to different degrees of polymerization. TGA revealed higher differences in the starting decomposition temperature, indicating different degrees polymerization corresponded to the light density distribution difference, i.e. the centre had a higher decomposition onset than the periphery. Similar results were obtained from DSC on the T_g, thus a significant decrease from 38 °C to around 1 °C were observed moving from the centre to the periphery. Control experiments of rocking the crosslinker-wetted element sulfur on an autonomous shaker for 12

h before submitting to the light irradiation, in order to try to improve mixing, gave a more

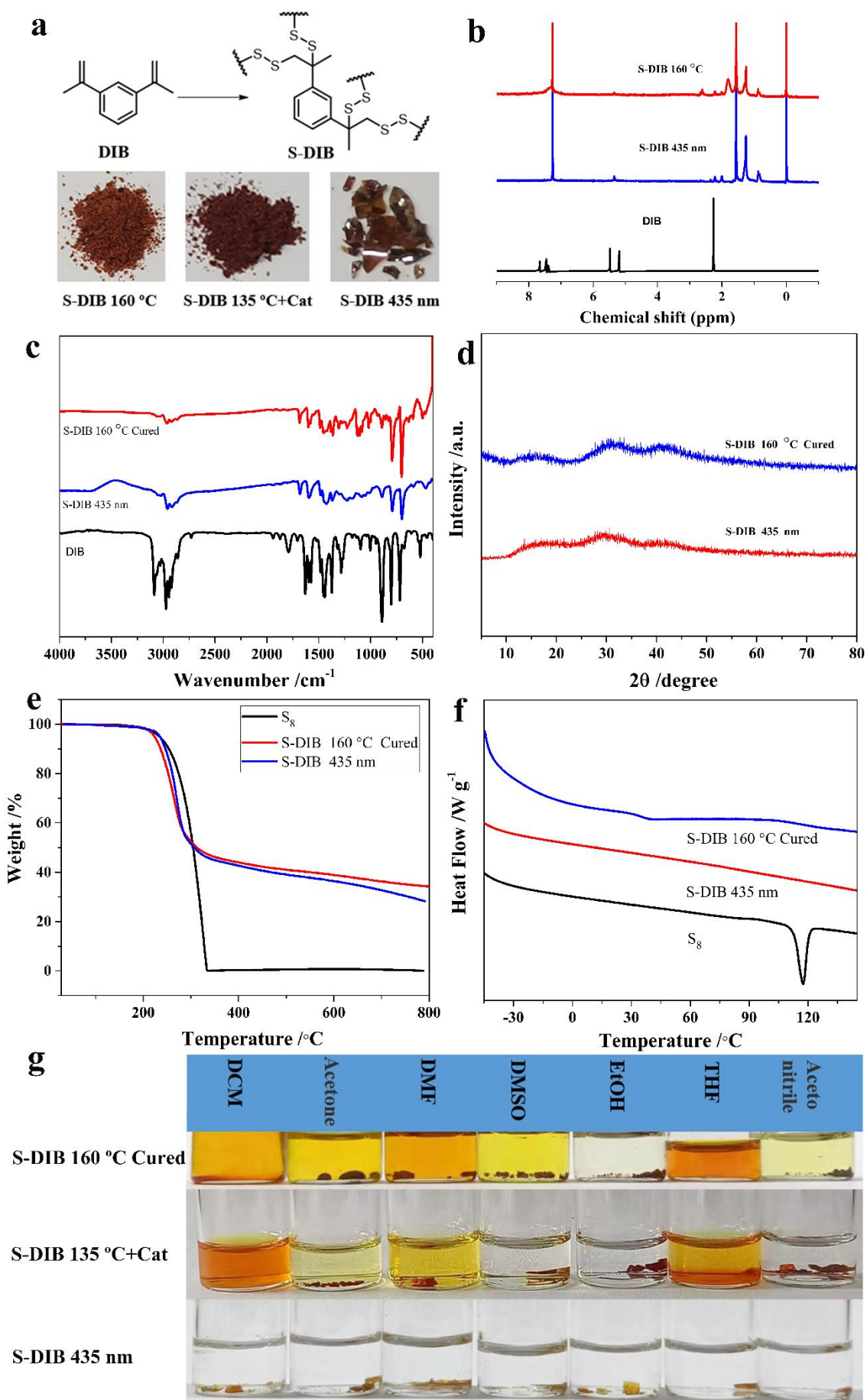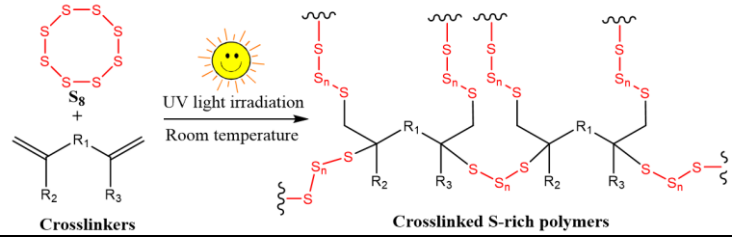uniform product (Figure S16, Extended Data Fig. 6f-i).

Figure 2. Photocatalytic inverse vulcanization (IV). (a) Scheme for synthesis of Poly(S-DIB) and photographs of polymers obtained by IV of S_8 with DIB under thermal (left and middle) and photocatalytic routes (right; 435 nm wavelength). (b) ^{1}H NMR of poly(S-DIB), from top to bottom: S_8 thermally reacted with DIB, S_8 photocatalytically reacted with DIB, and DIB crosslinker. (c) FT-IR of Poly (S-DIB) under different conditions of light and heating. (d) PXRD patterns of S_8 and Poly(S-DIB) obtained under different conditions. (e) TGA of S_8 (black) and Poly (S-DIB) from thermal reaction (red), photocatalytic reaction (blue). (f) DSC of S_8 (black) and Poly (S-DIB) produced thermally (blue) and photocatalytically (red). (g) Comparison of solubility of Poly (S-DIB) obtained under different conditions of heating (top), heating with Zn(TDC)$_2$ (middle), and light (435 nm) (bottom).

Initially, the polymers were cured in the oven overnight at 140 °C prior to characterization following the general procedure in the literature. However, the same spectrum was observed for the photocatalytic generated polymers without any cure procedure at all (either thermal or optical). This shows the extended curing stage is neither necessary nor beneficial for the further formation of the polymer, a significant saving in energy cost for production. As shown in Figures 2 and S5b-f, identical results were obtained by ^{1}H NMR, FTIR, PXRD, TGA, and DSC.

Validating previously reported crosslinkers. With the optimized photo-induced IV conditions in hand, the scope of the technique was tested across a range of crosslinkers (Extended Data Fig. 1a-c). As shown in Table 1, all the crosslinkers reported previously for both thermal and thermal catalytic conditions are feasible for the newly developed photo-induced IV process (Entries 1-15, Table S6, Figures in ESI for DSC/TGA/GPC/FTIR). In general, higher T_g, higher molecular weight (M_w), and lower PDI value were achieved compared to counterpart polymers produced under thermal conditions, indicating a more uniform structure.[50]

Table 1. Representative properties of photo-induced IV of S_8 with Petro-based and nature abundant crosslinkers reported previously.[a]

Entry	Crosslinkers[b]	Conditions	DSC[c]	GPC[d]		
			T_g / °C	M_n / gmol^{-1}	M_w / gmol^{-1}	PDI
1[e]	DIB	160 °C / 8 h	29.8	24,100	101,000	4.6
2[f]		135 °C Zn(DTC)$_2$ / 7 h	31.7	3100	3300	1.1
3		380 nm / 48 h	ND	165,000	243,000	1.5
4		435 nm / 6 h	ND	/	/	/
5	DCPD	435 nm / 6 h	ND	123,000	196,000	1.6
6	DADS	435 nm / 6 h	-13.4	48,300	116,000	2.4
7	VNB	435 nm / 6 h	1.3	248,000	334,000	1.4
8[g]	DEB	200 °C / 15 h	ND	5100	10200	2.0
9		435 nm / 6 h	ND	241,000	303,000	1.3
10	Myrcene	435 nm / 6 h	-15.5	55,700	131,000	2.4
11	Limonene	435 nm / 6 h	-14.9	55,600	154,000	2.8
12	Castor oil	435 nm / 6 h	-34.0	78,800	141,000	1.8

[a]: Reaction conditions: Without stirring, equal mass of elemental sulfur (50 mg, 0.195mmol) and crosslinkers (50 mg) were added to a photoreaction flask (quartz tube, 20 mL), and the reaction was carried out under 435 nm or 380 nm ultraviolet light (10 W) at room temperature for the time specified. The black solid obtained was then characterized by DSC, PXRD, *etc*. [b]: DIB = 1,3-diisopropenylbenzene; DCPD = Dicyclopentadiene; DEB = 1,3-diethynylbenzene; VNB = 5-vinylbicyclo[2.2.1]hept-2-ene; DADS = Diallyldisulfide; [c]: ND = Not Detected. [d]: DMF was used as solvent. Please refer to ESI for detailed GPC conditions and results. [e]: Equal mass of 0.5 g of S_8 and DIB were reacted, for detailed reaction conditions please see ESI. [f]: Equal mass of 0.5 g of S_8 and DIB were reacted in the present of Zn(DTC)$_2$ (3 mg), for detailed reaction conditions please see ESI. [g]: Equal mass of 0.5 g of S_8 and DEB were reacted, for detailed reaction conditions please see ESI.

Alkyne bonds have been explored previously in the IV reaction under thermal conditions, although only for a single crosslinker, 1,3-diethynylbenzene (DEB).[11,51] That sulfur-DEB reaction required heating to over 200 °C to proceed. By contrast, the same reaction can be realized by photo-induced IV at room temperature (Figure S18), providing poly(S-DEB) with much higher M_w (M_w 303,000 gmol^{-1} with PDI of 1.3 to M_w 10,200 gmol^{-1} with PDI of 2.0) compared to its thermal counterpart (Entry 9 *vs* 8, Table 1). The IV of S_8 with phenylacetylene (PA) was also achieved by this protocol (Figure S19), affording fully soluble polymers with M_w of 264,000 gmol^{-1}, PDI of 1.3, and high S content of 50.6% (Entry 5, Table S6). The partial solubility of many of the photo-induced IV products suggest some linear rather than

fully crosslinked character, potentially resulting from an increased propensity for intramolecular reaction and sulfur loops. All the polymers generated by this photo-induced IV with aforementioned crosslinkers have been fully characterized (Figures in ESI).

Crosslinkers of low boiling point alkenes. Ambient temperature reaction allows the substrate scope of the IV reaction to be expanded to very low boiling point alkenes for the first time, affording sulfur-rich polymers which could not be made otherwise without requiring complex high-pressure equipment. A series of photo-induced IV reactions proceeded efficiently for crosslinkers of low boiling point alkenes, such as diallylamine (DAA, BP: 111 °C), 2,3-dimethylbuta-1,3-diene (DMBD, BP: 68 °C), isoprene (IP, BP: 34 °C), and 2-methylbut-1-en-3-yne (MBEY, BP: 33 °C) with S_8, affording S-rich polymers in near quantative yields (Figures 3a, c; Entries 1-4, Table S7, Extended Data Fig. 1b). ^{1}H NMR spectra show either complete, or close to complete, conversion of the alkene bonds in these crosslinkers. DSC traces indicate the crystalline S_8 has reacted with all of these crosslinkers (Table S7, Figures S29-S36, S71-S78). In general, most of these polymers had a soluble fraction between 16-70 wt.% in DMF, while some of them are completely soluble in DMF, such as poly(S-CO), poly(S-PA) and poly(S-DAA) (Table S8, Figures S98-99, Extended Data Fig. 3b-e). Similarly, high molecular weights (up to 463,000 gmol^{-1}) with the PDI value closed to 1 show an increase in linear character of the soluble fraction (Entries 11-13, Table S6). These polymers show high thermal stabilities (>200 °C) as evidenced by the TGA analysis (Figure S55, Extended Data Fig. 8) and FTIR proved the transformation of covalent C=C bonds in the new S-rich polymers (Figures S38-S53).
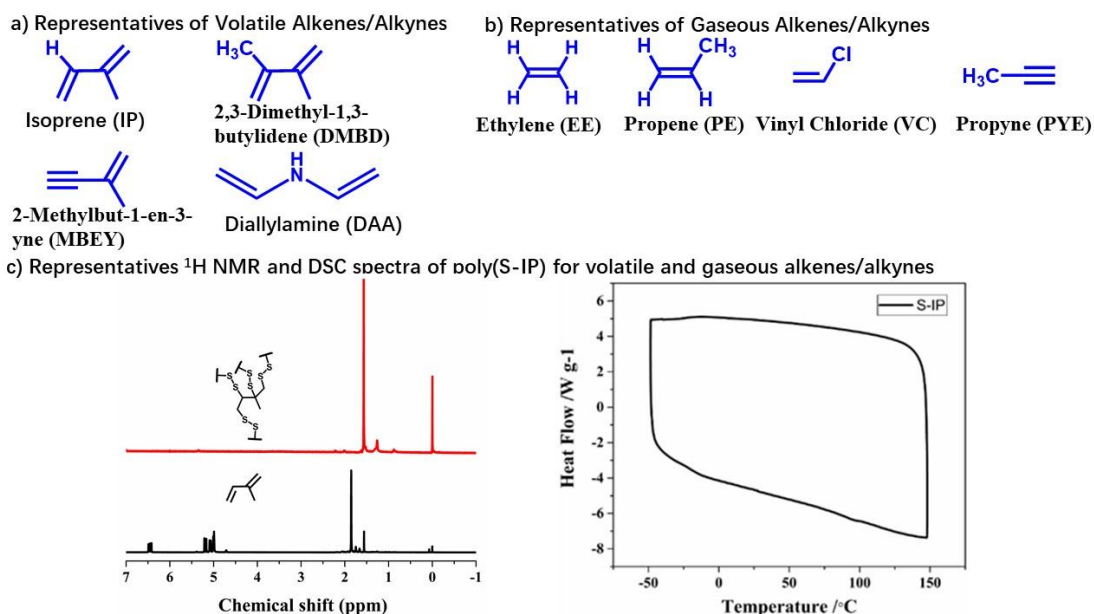
Figure 3. Representative of crosslinkers/comonomers of low boiling point alkenes and alkynes (a), gaseous comonomers (b), and ^{1}H NMR and DSC spectra of obtained S-rich polymers for poly(S-IP) (c).

Co-monomers and crosslinkers of gaseous alkenes and alkynes. The photocatalytic protocol even enables more abundant and less expensive gaseous alkenes and alkynes to be used in the IV reaction for the first time. Gaseous comonomers, such as ethylene (EE), propene (PE), propyne (PYE), and vinyl chloride (VC) were inverse vulcanized with S_8 under 1 atm induced by UV at 435 nm (Figure 3b, Extended Data Fig. 1c). It should be noted that a small amount (20 µL) of toluene was sprayed on the surface of S_8 in order to aid and enhance the diffusion process of these gaseous molecules. The photo-induced IV reaction of S_8 with the gaseous comonomers was successful (Entries 5-8, Table S7). ^{1}HNMR and DSC results demonstrated full conversion for each of the IV reactions with these gaseous comonomers, except for some unreacted crystalline S_8 detected in DSC traces for both EE and PE (Table S7; Figures S74-75). These polymers were very stable and there was no colour change for more than a year in these materials, demonstrating no further precipitation of S_8. Reaction of the double or triple bond and the formation of the C-S bond was confirmed spectroscopically (Table S7; Figures S32-S33,), including FTIR (Figures S50-51). The gaseous comonomers produced high sulfur

content polymers that were soluble well in DMF (Table S8, Figures S98-99) with very high M_w and low PDI; *e.g.*, 289,000 gmol^{-1} (PDI, 1.2) for EE, 117,000 gmol^{-1} (PDI, 2.1) for PE, 428,000 gmol^{-1} (PDI, 1.1) for acetylene (ACE), and 317,000 gmol^{-1} (PDI, 1.4) for PYE, respectively (Entries 14-18, Table S6). The absence of peaks in the PXRD patterns for these polymers indicates that the crystalline S_8 was fully reacted (Figure S54, Extended Data Fig. 7). The elemental analysis results of poly(S-PYE) indicated sulfur content of 92.6% (Entry 14, Table S6). This is a high proportion of sulfur that is stabilised against depolymerisation, but this can be rationalized by the relatively high ratio of reactive bonds on propyne based on its molecular mass. Similar results were achieved for IV with other gaseous comonomers, including EE, PE, and VC (Entries 15-17, Table S6). A key advantage of this photoreaction process is to bring low boiling point alkenes as well as gaseous crosslinkers into inverse vulcanization routes, thus greatly expanding the family of S-rich polymers and their potential applications.

The scale of the protocol presented here is limited by the size of reactor rather than the chemistry itself. By using a larger reactor, multi gram S-rich polymers were obtained with the same quality and quantitative yield (Figure S17).

Given the simple operation and mild conditions, a further advantage of this protocol is that S-rich polymers can be *in situ* polymerized as coatings onto the surface of substrates without any additional processing steps. This could allow IV polymers to be used with existing industrial processes such as photo-activated screen printing.[52-54] As a demonstration, poly(S-DIB) was reactively coated onto the surface of filter paper (Figures S100-102, Extended Data Fig. 9). FTIR and DSC confirmed the completion of the polymerization, while SEM and EDS images demonstrated an even S-rich polymer coating.

One promising application of IV polymers is in mercury capture and remediation.[16-17] Photoinduced IV polymers were therefore tested for this application to check whether they retained mercury capture properties when produced by this route. Gratifyingly, the photoinduced S-rich polymers showed comparable or better adsorption rates and sorbent capacities for mercury uptake as compared to materials produced by thermal reactions (Figures S103-105).

Mechanistic investigation

Both free radical and anionic mechanisms have been proposed in the literature for the IV reaction under thermal conditions, as was concerted pathway for IV involving metal catalysts.[4-5,8-9,18,50,55] It is most likely that a free radical mechanism is in operation in photo-induced IV because free radicals will be generated easily, and in preference to ions, by adventitious homolytic bond cleavage of S_8 under light irradiation. The key factor in this mechanism is the promotion of both S_8 and the crosslinkers from their ground states to excited states by light absorption, both minimizing the transition energy (ΔG^+) of the original reaction and also encouraging the interaction of excited states of reactants through an altered pathway, which allows the polymerization to occur at room temperature.

Investigations into the rate-determining step were attempted before exploring the mechanism. UV-visible light absorption by the reactants is pivotal for the photo-induced IV to occur and proceed, and this was quantified for both S_8 and the crosslinkers, as shown in Figure S106. In agreement with the absorption onset for S_8 of 475 nm at room temperature,[56] S_8 shows a broad band light absorption up to 520 nm wavelength and the strongest absorption between 380 nm and 435 nm, whereas the crosslinker absorptions band are mainly located below 320 nm in the UV. We found that with irradiation at wavelengths above 520 nm there was no reaction. At

435 nm the reaction proceeds, and at 380 nm the reaction proceeds more slowly, possibly due to competing reactions. This lack of reaction under photoirradiation with light of 520 nm or above suggests an essential energy requirement for photoinduced ring opening of S_8.

At 435 nm, the reaction occurred between DIB and sulfur chains after ring-opening of S_8 by visible light, affording typical black S-rich polymers as the product. There was a long induction time for the model reaction under 380 nm light irradiation with significant amounts of unreacted DIB presence after 24 h (Figures 2b, S5, S8). One explanation for this is that the high energy of UV light at 380 nm both ring-opens S_8 but also accelerates the self-polymerization of sulfur to generate linear polymeric pure sulfur. The pure-sulfur polymer could then be decomposed *in situ* back to S_8 and ring-opened again by the UV light, therefore adding a reversible reaction that competes with IV. This is supported by Raman spectroscopy observations that S_8 can ring open and polymerize when subject to 325 nm irradiation.[52] Pure polymeric sulfur would also explain the golden-orange to orange-red color of the polymer obtained under these conditions. Another possibility is that reactants could be excited to their more short-lived triplet state, which have less chance to react. The reason for homopolymerisation of S_8 detracting from copolymerization for the photoinduced more than the thermally induced reaction could potentially be linked to the differences in diffusion/agitation. The thermal reactions are normally vigorously stirred, allowing a greater rate of mixing. Without such agitation in the photoinduced route, it relies on a generated sulfur radical having chance to diffuse and contact an organic molecule. Too high a level of homopolymerization could slow diffusion and mixing.

The IV of S_8 with DIB in the presence of $Zn(DTC)_2$ catalyst still required a temperature of 100-135 °C, indicating there a significant activation energy barrier to overcome, even with this catalyst. By contrast, the equivalent photopolymerization proceeds at room temperature, demonstrating that this barrier probably exists prior to the C-S bond formation. These results

strongly suggested that the ring-opening of S_8 is the rate-determining step in the IV reaction.

Based on this insight into the rate-determining step, we speculated on a conceivable reaction mechanism. It is known that S_8 has two distinct electronic transitions relating to visible and UV light, resulting a narrow indirect bandgap and a wide direct bandgap, respectively.[56] The former is phonon dependent requiring sufficient temperature to generate phonons, where the latter is a phonon-independent process. Effective electronic transition only occurred in the UV-excited direct mode. Therefore, cleavage of S-S bonds requires activation by UV light. Neither the S_8 nor the crosslinkers homopolymerize under the photo-induced IV conditions at room temperature. Almost all the crosslinkers tested reacted smoothly with S_8 under this protocol. However, EGDMA required extra photosensors or dyes to produce corresponding S-rich polymers with UV light, even in the presence of metal co-catalysts. EGDMA is a problematic crosslinker for IV under thermal conditions without the aid of catalyst, indicating a high energy barrier. This is also the case for this photo-induced IV method; there is almost no reaction under the general optimized photo conditions with 435 nm wavelength light, requiring extra energy to overcome a high active energy barrier with 380 nm wavelength light and a long reaction time of 48 h in the presence of the photosensor ethyl eosin (Figure S107). DFT calculations show that the energy barrier for the excited state of EGDMA is about 6.00 eV (Figure S115); that is, much higher than the light could provide (3.26 eV for 380 nm, and 2.85 eV for 435 nm). These also support the ring-opening of S_8 being the rate-determine step for most of the crosslinkers, and suggests a generalized reaction pathway (Figure S108). After the reactants are promoted to their excited states by light irradiation, S_8 is ring-opened by light irradiation to generate the sulfur free radicals, which then attack the weaker or lower activation energy covalent C=C bonds in the crosslinkers/comonomers. This requires additional energy or photosensitization for substrates with high transition energy barriers, such as EGDMA. This

also explains the sluggish IV reaction with acetylene. A light-induced radical mechanism is further supported by the findings of *in situ* UV-irradiated electron paramagnetic resonance (EPR) measurements, that showed the presence of radicals when elemental sulfur is irradiated with UV light.[56]

It is noteworthy that a lower molecular weight of poly(S-DIB) prepared with catalyst under thermal conditions was observed, presumably due to the active intermediates generated by the Zinc catalysts. That is, with the addition of catalyst $Zn(DTC)_2$, the formation rate of sulfur radical is accelerated and the degree of polymerization is reduced.

Theoretical calculations provided further support for the proposed mechanism. As mentioned above, the ring-opening of S_8 was expected to be the rate-determining step for the overall IV polymerization for DIB. A plausible reaction pathway for the formation of Poly(S-DIB) by S_8 with DIB under three different conditions was calculated, as shown in Figures 4 and S109-115 (Extended Data Fig. 10).[55] First, in the absence of $Zn(DTC)_2$ co-catalyst and light irradiation, it was found that the ring-opening of S_8 needs to overcome a barrier of 0.55 eV to form the active sulfur species. However, the S_8 ring-opening activation must overcome a barrier of just 0.22 eV when the $Zn(TDC)_2$ co-catalyst is introduced, indicating that the activity of S_8 can be significantly improved through the altered catalytic route. These calculations suggest that the S_8 ring-opening can occur by light irradiation only under its excited state, which would directly generate excited sulfur radicals and the corresponding excited states were calculated at the M06-2X level for better accuracy. These sulfur radicals can attack the light-activated carbon atoms in the C=C bonds of DIB to generate the poly(S-DIB)s, and this reaction is exothermic by about 4.90 eV. This supports our mechanistic explanation for photo-induced catalytic IV occurring at room temperature with a different catalytic pathway, and the DFT calculation results are consistent with the experimental observations.
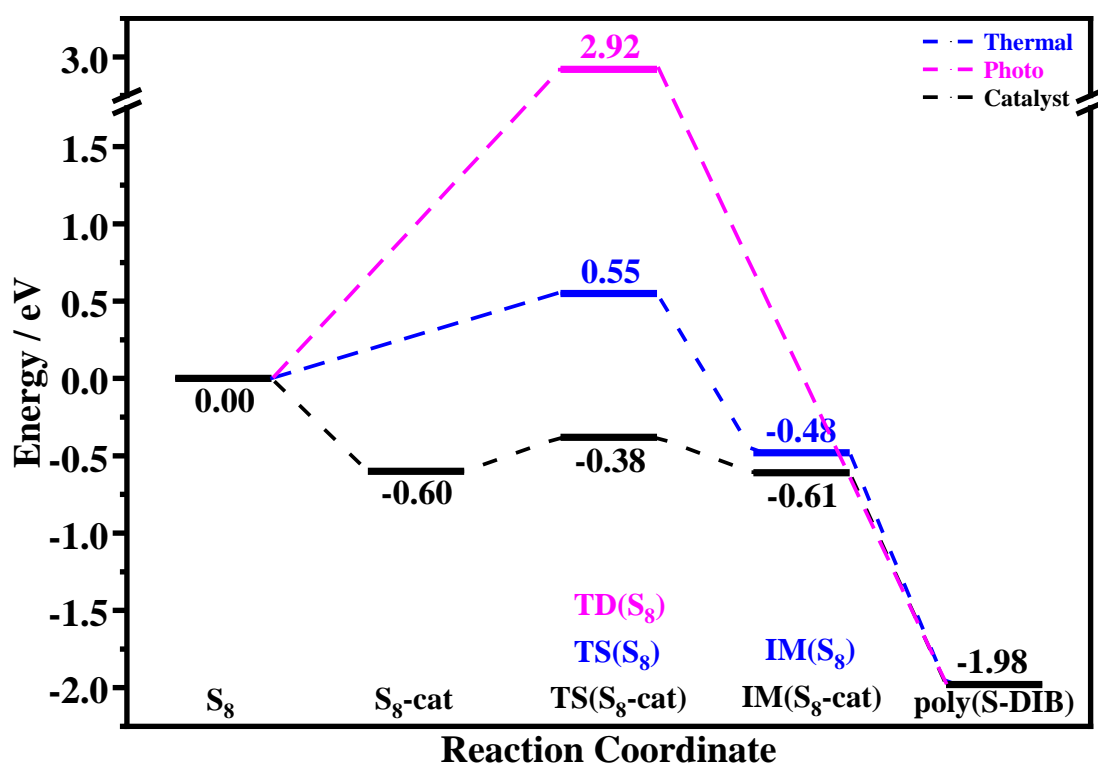
Figure 4. Calculated energy profiles for the formation of Poly(S-DIB) by S_8 with DIB under various conditions (TD = Excited State; TS = Transition State; IM = Intermediate State). The blue route corresponds to a thermal process, the black one is under the influence of the $Zn(DTC)_2$ co-catalyst, and the pink one is photo-promoted. Detailed calculations and key structures are also presented in Figures S109-115 (Extended Data Fig. 10).

Conclusions

Photo-induced IV offers a more sustainable and cleaner platform for the IV reaction of S_8 with a diverse variety of crosslinkers that cannot be used through thermal routes. This addresses multiple challenges in this area, including the scope of crosslinkers, the diversity of the synthetic method, the energy consumption of the reaction (*e.g.*, in scale up), and the breadth of properties attainable in these S-rich polymers. The advantages of this photo-induced IV polymerization method are: i) very mild conditions of room temperature (18-20 °C); ii) greatly broadened scope of crosslinkers, including low boiling point alkenes, alkynes as well as even cheaper and more abundant gaseous crosslinkers (*e.g.*, ethylene, propene, acetylene, propyne *etc.*); iii) avoidance of an extended heated curing step; iv) no generation of toxic H_2S gas by-

products; v) no requirement for metal co-catalysts in most cases; and vi) no auto acceleration of the polymerization, which is a common problem for thermal routes. The molecular weights (M_w) of the photopolymerized polymers could reach up to 460,000 gmol^{-1} with narrow PDI values of 1-1.5. The S-rich polymers generated with volatile and gaseous co-monomers are not easily obtained by any other routes, which affords potentially sustainable alternatives to environmentally problematic plastics. We propose a mechanism for the photopolymerization, supported by experimental and computational results, which suggests that photo-induced IV operates via a different pathway compared to established thermal IV reactions. This protocol is both a significant step forward in the fundamental chemistry of IV and also greatly enhances the prospects for industrial commercialization of IV polymers as sustainable alternatives for environmentally harmful commodity plastics in the future.

Methods:

All chemicals were used as received.
The photo-induced IV reaction was carried out in a WATTCAS^{TM} photoreactor equipped with the quartz glass tube (20 mL, inner diameter 1.6 cm) contained in an open-bottom steel sleeve with cap (Figure S1). The light beam (10 W) comes from the bottom of the reaction tube and the distance is 0.5 cm. The liquid organic crosslinkers were completely absorbed by the element sulfur powder and the resulted solid mixture was laid out as a very thin layer, the thinner the better, at the bottom of the flask in order to get sufficient light irradiation. The specific wavelength of light is controlled by optical chip provided by WATTCAS^{TM}.

Representative standard procedure for the preparation of S-rich polymers under thermal, thermal + catalysts, and light conditions, for more details please see supporting information:

Preparation of Poly(S-DIB) under the condition of 135 °C plus catalyst: A 500 mg (1.95 mmol) of S_8 and the catalyst zinc diethyldithiocarbamate (3 mg, 0.0082 mmol) were added into a 25 mL tube with magnetic stir bar. After heating to a molten state at 120 °C, 500 mg (3.1 mmol) DIB was added, the mixture was reacted at 135 °C for 12 h. After cooled down to room temperature, the product was cured in vacuum oven at 140 °C for 12 h. A crimson solid was obtained. PXRD and DSC found that there is no unreacted sulfur in Poly(S-DIB).

Preparation of Poly(S-DIB) at 160 °C using traditional thermal method: A 500 mg (1.95 mmol) of S_8 was added into a 25 mL tube with magnetic stir bar, after heating at 120 °C to a molten state, 500 mg (3.1 mmol) of DIB was added and the mixture was reacted at 160 °C for 12 h. After cooled down to room temperature, the product was cured in vacuum oven at 140 °C for 12 h. A crimson solid was obtained. PXRD and DSC found that there is no unreacted sulfur in Poly(S-DIB).

Preparation of Poly(S-DIB) under 380 nm light conditions in the present of Zn(DTC)$_2$: Without a magnetic stir bar, the equal mass of elemental sulfur (50 mg, 0.195 mmol) and DIB (50 mg, 0.31 mmol) were added into a 20 mL photoreaction flask (quartz tube) with Zn(DTC)$_2$ (3 mg, 0.0082 mmol), the reaction was carried out at room temperature under 380 nm ultraviolet light for 48 hours. A golden to golden-orange solid was obtained. PXRD and DSC found that there is no unreacted sulfur in Poly(S-DIB).

Preparation of Poly(S-DIB) under 380 nm light conditions: Without a magnetic stir bar, the equal mass of elemental sulfur (50 mg, 0.195 mmol) and DIB (50 mg, 0.31 mmol) were added into a 20 mL photoreaction flask

(quartz tube), the reaction was carried out at room temperature under 380 nm ultraviolet light for 48 hours. A golden-red to orange-red solid was obtained. PXRD and DSC found that there is no unreacted sulfur in Poly(S-DIB).

Preparation of Poly(S-DIB) under 435 nm light conditions: Without a magnetic stir bar, the equal mass of elemental sulfur (50 mg, 0.195 mmol) and DIB (50 mg, 0.31 mmol) were added into a 20 mL photoreaction flask (quartz tube), the reaction was carried out at room temperature under 435 nm ultraviolet light for 6 hours. A black solid was obtained. The resultant polymers were recovered manually by scraping out the solid product with a spatula, and characterized without further purification or curation. 95.2 mg of the product was obtained and the yield is 95.2%. PXRD and DSC found that there is no unreacted sulfur in Poly(S-DIB).

Theoretical Calculations: First-principles calculations were performed to better illuminate the IV reaction mechanism under various conditions. The energy profiles of the synthesis of poly(S-DIB) were determined by the spin-unrestricted density functional theory (DFT) calculations using the Gaussian 16 program package.[57] All structures and energies were optimized without symmetry constrains at the B3LYP [58-59] level, and the Lanl2DZ basis set[60] for Zn and the 6-311G* basis set[61] for H, C, N, S were used. To simulate the reaction of DIB and EGDMA with S_8 under the light irradiation, the excited states of S_8, DIB, and EGDMA have been investigated in the framework of time-dependent density functional theory (TD-DFT),[62] and the corresponding excited states were calculated at the M06-2X level.[63]

Note on crosslinker/monomer terminology: A crosslink is a point in a polymer where chains extend in four directions. In conventional vulcanization, the sulfur is thought of as the crosslinker because the organic polymer forms the linear sections, with the sulfur then reacting to join two chains together (and hence four sections extending from that point). With inverse vulcanization, the organic component is usually a small molecule itself rather than a polymer. Most often one with two double bonds. These can react with the sulfur to form a section that has four linear sulfur chains extending from it. As such, it is the organic component in inverse vulcanization that is often referred to as the crosslinker. In the manuscript, we refer to the organic molecules that are reacted with sulfur as "monomers" in the cases where they only have one double bond, as they would be expected to form linear polymers, and "crosslinkers" in the cases where they have two or more double bonds, as they would be expected to form crosslinked polymers.

Data availability: The authors declare that the data supporting the findings of this study are available within the paper and its supplementary information files. Should any raw data files be needed in another format they are available from the corresponding author upon reasonable request.

Author contributions

Z-J.Q., X.F.W., and T.H. conceived the project. J.H.J. carried out the experimental works. J.H.J. and J.J. L. performed the characterizations. X.Q.G., L.J.C., X.F.W., and T.H. conceived the computational simulations strategy. Z.Q.W., T.L., and C.X.Z. performed the calculations. P.Y.Y., W.Z., C.C.M., and S.S.C. carried out the control reactions, parallel experiments, in situ coating experiments, Hg adsorption,

and performed the characterizations. X-C.W. accessed FTIR, GPC spectra and confirmed the data. A.I.C. discussed the results and thoroughly revised the manuscript. All authors interpreted the data and contribute to the preparation of the manuscript.

Competing interests
The authors declare no competing interests.

Additional information
Supplementary information is available for this paper at

Correspondence and requests for materials should be addressed to TH, XFW, AIC, or ZJQ

References

1. Boyd DA. Sulfur and Its Role In Modern Materials Science. *Angew. Chem. Int. Ed.* 2016, **55**(50): 15486-15502.

2. Griebel JJ, Glass RS, Char K, Pyun J. Polymerizations with elemental sulfur: A novel route to high sulfur content polymers for sustainability, energy and defense. *Prog. Polym. Sci.* 2016, **58**: 90-125.

3. Kohl AIN, R.B.; . Sulfur Recovery Processes. *Gas Purification*, 5th ed. edn. Gulf Publishing: Houston, TX, 1997, pp 670-730.

4. Worthington MJH, Kucera RL, Chalker JM. Green chemistry and polymers made from sulfur. *Green Chem.* 2017, **19**(12): 2748-2761.

5. Zhang YY, Glass RS, Char K, Pyun J. Recent advances in the polymerization of elemental sulphur, inverse vulcanization and methods to obtain functional Chalcogenide Hybrid Inorganic/Organic Polymers (CHIPs). *Polym. Chem.* 2019, **10**(30): 4078-4105.

6. Zhu YQ, Romain C, Williams CK. Sustainable polymers from renewable resources. *Nature* 2016, **540**(7633): 354-362.

7. Choi JW, Aurbach D. Promise and reality of post-lithium-ion batteries with high energy densities. *Nat. Rev. Mater.* 2016, **1**(4): 16013.

8. Chalker JM, Worthington MJH, Lundquist NA, Esdaile LJ. Synthesis and Applications of Polymers Made by Inverse Vulcanization. *Top. Curr. Chem.* 2019, **377**(3).

9. Chung WJ, Griebel JJ, Kim ET, Yoon H, Simmonds AG, Ji HJ, *et al.* The use of elemental sulfur as an alternative feedstock for polymeric materials. *Nat. Chem.* 2013, **5**(6): 518-524.

10. Griebel JJ, Namnabat S, Kim ET, Himmelhuber R, Moronta DH, Chung WJ, *et al.* New Infrared Transmitting Material via Inverse Vulcanization of Elemental Sulfur to Prepare High Refractive Index Polymers. *Adv. Mater.* 2014, **26**(19): 3014-3018.

11. Dirlam PT, Simmonds AG, Kleine TS, Nguyen NA, Anderson LE, Klever AO, *et al.* Inverse

vulcanization of elemental sulfur with 1,4-diphenylbutadiyne for cathode materials in Li-S batteries. *Rsc Adv.* 2015, **5**(31): 24718-24722.

12.   Zhang YY, Griebel JJ, Dirlam PT, Nguyen NA, Glass RS, Mackay ME*, et al.* Inverse vulcanization of elemental sulfur and styrene for polymeric cathodes in Li-S batteries. *J. Polym. Sci. A Polym. Chem.* 2017, **55**(1): 107-116.

13.   Zhang YY, Konopka KM, Glass RS, Char K, Pyun J. Chalcogenide hybrid inorganic/organic polymers (CHIPs) via inverse vulcanization and dynamic covalent polymerizations. *Polym. Chem.* 2017, **8**(34): 5167-5173.

14.   Kwon M, Lee H, Lee SH, Jeon HB, Oh MC, Pyun J*, et al.* Dynamic Covalent Polymerization of Chalcogenide Hybrid Inorganic/Organic Polymer Resins with Norbornenyl Comonomers. *Macromol. Res.* 2020, **28**(11): 1003-1009.

15.   Crockett MP, Evans AM, Worthington MJH, Albuquerque IS, Slattery AD, Gibson CT*, et al.* Sulfur-Limonene Polysulfide: A Material Synthesized Entirely from Industrial By-Products and Its Use in Removing Toxic Metals from Water and Soil. *Angew. Chem. Int. Ed.* 2016, **55**(5): 1714-1718.

16.   Worthington MJH, Kucera RL, Albuquerque IS, Gibson CT, Sibley A, Slattery AD*, et al.* Laying Waste to Mercury: Inexpensive Sorbents Made from Sulfur and Recycled Cooking Oils. *Chem. Eur. J.* 2017, **23**(64): 16219-16230.

17.   Tikoalu AD, Lundquist NA, Chalker JM. Mercury Sorbents Made By Inverse Vulcanization of Sustainable Triglycerides: The Plant Oil Structure Influences the Rate of Mercury Removal from Water. *Adv. Sustain. Syst.* 2020, **4**(3).

18.   Wu XF, Smith JA, Petcher S, Zhang BW, Parker DJ, Griffin JM*, et al.* Catalytic inverse vulcanization. *Nat. Commun.* 2019, **10**: 647.

19.   Smith JA, Green SJ, Petcher S, Parker DJ, Zhang BW, Worthington MJH*, et al.* Crosslinker Copolymerization for Property Control in Inverse Vulcanization. *Chem. Eur. J.* 2019, **25**(44): 10433-10440.

20.   Parker DJ, Jones HA, Petcher S, Cervini L, Griffin JM, Akhtar R*, et al.* Low cost and renewable sulfur-polymers by inverse vulcanisation, and their potential for mercury capture. *J. Mater. Chem. A* 2017, **5**(23): 11682-11692.

21.   Smith JA, Wu XF, Berry NG, Hasell T. High Sulfur Content Polymers: The Effect of Crosslinker Structure on Inverse Vulcanization. *J. Polym. Sci. A Polym. Chem.* 2018, **56**(16): 1777-1781.

22.   Hoefling A, Lee YJ, Theato P. Sulfur-Based Polymer Composites from Vegetable Oils and Elemental Sulfur: A Sustainable Active Material for Li-S Batteries. *Macromol. Chem. Phys.* 2017, **218**(1): 9.

23.   Hoefling A, Nguyen DT, Lee YJ, Song SW, Theato P. A sulfur-eugenol allyl ether copolymer: a material synthesized via inverse vulcanization from renewable resources and its application in Li-S batteries. *Mat. Chem. Front.* 2017, **1**(9): 1818-1822.

24.   Duarte ME, Huber B, Theato P, Mutlu H. The unrevealed potential of elemental sulfur for the synthesis of high sulfur content bio-based aliphatic polyesters. *Polym. Chem.* 2020, **11**(2): 241-248.

25.   Scheiger JM, Direksilp C, Falkenstein P, Welle A, Koenig M, Heissler S, *et al.* Inverse Vulcanization of Styrylethyltrimethoxysilane-Coated Surfaces, Particles, and Crosslinked Materials. *Angew. Chem. Int. Ed.* 2020, **59**(42)**:** 18639-18645.

26.   Gomez I, Mecerreyes D, Blazquez JA, Leonet O, Ben Youcef H, Li CM, *et al.* Inverse vulcanization of sulfur with divinylbenzene: Stable and easy processable cathode material for lithium-sulfur batteries. *J. Power Sour.* 2016, **329:** 72-78.

27.   Gomez I, Leonet O, Blazquez A, Mecerreyes D. Exploring inverse vulcanization of sulfur with natural source monomers as cathodic materials for long life lithium sulfur batteries. *Abstr. Pap. Am. Chem. Soc.* 2017, **253:** 1.

28.   Gomez I, Leonet O, Blazquez JA, Grande HJ, Mecerreyes D. Poly(anthraquinonyl sulfides): High Capacity Redox Polymers for Energy Storage. *ACS Macro. Lett.* 2018, **7**(4)**:** 419-424.

29.   Thiounn T, Lauer MK, Bedford MS, Smith RC, Tennyson AG. Thermally-healable network solids of sulfur-crosslinked poly(4-allyloxystyrene). *Rsc Adv.* 2018, **8**(68)**:** 39074-39082.

30.   Lauer MK, Estrada-Mendoza TA, McMillen CD, Chumanov G, Tennyson AG, Smith RC. Durable Cellulose-Sulfur Composites Derived from Agricultural and Petrochemical Waste. *Adv. Sustain. Syst.* 2019, **3**(10): 1900062.

31.   Karunarathna MS, Lauer MK, Smith RC. Facile route to an organosulfur composite from biomass-derived guaiacol and waste sulfur. *J. Mater. Chem. A* 2020, **8**(39)**:** 20318-20322.

32.   Karunarathna MS, Tennyson AG, Smith RC. Facile new approach to high sulfur-content materials and preparation of sulfur-lignin copolymers. *J. Mater. Chem. A* 2020, **8**(2)**:** 548-553.

33.   Diez S, Hoefling A, Theato P, Pauer W. Mechanical and Electrical Properties of Sulfur-Containing Polymeric Materials Prepared via Inverse Vulcanization. *Polym.* 2017, **9**(2): 59.

34.   Arslan M, Kiskan B, Cengiz EC, Demir-Cakan R, Yagci Y. Inverse vulcanization of bismaleimide and divinylbenzene by elemental sulfur for lithium sulfur batteries. *Eur. Polym. J.* 2016, **80:** 70-77.

35.   Kleine TS, Nguyen NA, Anderson LE, Namnabat S, LaVilla EA, Showghi SA, *et al.* High Refractive Index Copolymers with Improved Thermomechanical Properties via the Inverse Vulcanization of Sulfur and 1,3,5-Triisopropenylbenzene. *ACS Macro. Lett.* 2016, **5**(10)**:** 1152-1156.

36.   Zhang YY, Kleine TS, Carothers KJ, Phan DD, Glass RS, Mackay ME, *et al.* Functionalized chalcogenide hybrid inorganic/organic polymers (CHIPs) via inverse vulcanization of elemental sulfur and vinylanilines. *Polym. Chem.* 2018, **9**(17)**:** 2290-2294.

37.   Gomez I, De Anastro AF, Leonet O, Blazquez JA, Grande HJ, Pyun J, *et al.* Sulfur Polymers Meet Poly(ionic liquid)s: Bringing New Properties to Both Polymer Families. *Macromol. Rap. Commun.* 2018, **39**(21): 1800529.

38.   Omeir MY, Wadi VS, Alhassan SM. Inverse vulcanized sulfur-cycloalkene copolymers: Effect of ring size and unsaturation on thermal properties. *Mater. Lett.* 2020, **259**(4)**:** 126887.

39.   Gomez I, Leonet O, Blazquez JA, Mecerreyes D. Inverse Vulcanization of Sulfur using Natural

Dienes as Sustainable Materials for Lithium-Sulfur Batteries. *ChemSusChem* 2016, **9**(24)**:** 3419-3425.

40. Parker DJ, Chong ST, Hasell T. Sustainable inverse-vulcanised sulfur polymers. *Rsc Adv.* 2018, **8**(49)**:** 27892-27899.

41. Shukla S, Ghosh A, Sen UK, Roy PK, Mitra S, Lochab B. Cardanol benzoxazine-Sulfur Copolymers for Li-S batteries: Symbiosis of Sustainability and Performance. *ChemSelect* 2016, **1**(3)**:** 594-600.

42. Lopez CV, Karunarathna MS, Lauer MK, Maladeniya CP, Thiounn T, Ackley ED*, et al.* High strength,acid-resistantcomposites from canola, sunflower, or linseed oils: Influence of triglyceride unsaturation on material properties. *J. Polym. Sci.* 2020, **58**(16)**:** 2259-2266.

43. Herrera C, Ysinga KJ, Jenkins CL. Polysulfides Synthesized from Renewable Galic Components and Repurposed Sulfur Form Environmentally Friendly Adhensives. *Acs Appl. Mater. Interfaces* 2019, **11**(38): 35312-35318.

44. Kang H, Kim H, Park MJ. Sulfur-Rich Polymers with Functional Linkers for High-Capacity and Fast-Charging Lithium-Sulfur Batteries. *Adv. Energy Mater.* 2018, **8**(32): 1802423.

45. Zhang YY, Pavlopoulos NG, Kleine TS, Karayilan M, Glass RS, Char K*, et al.* Nucleophilic Activation of Elemental Sulfur for Inverse Vulcanization and Dynamic Covalent Polymerizations. *J. Polym. Sci. A Polym. Chem.* 2019, **57**(1)**:** 7-12.

46. Zhang YY, Konopka KM, Glass RS, Char K, Pyun J. Chalcogenide Hybrid Inorganic/Organic Polymers (CHIPs) via Inverse Vualcanization and Dynamic Colvanent Polymerizations. *Polym. Chem.* 2017, **8**, 5167-5173.

47. Westerman CR, Jenkins CL. Dynamic Sulfur Bonds Initiate Polymerization of Vinyl and Allyl Ethers at Mild Temperatures. *Macromolecules* 2018, **51**(18), 7233-7238.

48. Dodd LJ; Omar O; Wu XF HT. Investigating the Role and Scope of Catalysts in Inverse Vulcanization. *ACS Catal.* 2021, **11:** 4441-4455.

49. Tian T, Hu RR, Tang BZ. Room Temperature One-Step Conversion from Elemental Sulfur to Functional Polythioureas through Catalyst-Free Multicomponent Polymerizations. *J. Am. Chem. Soc.* 2018, **140**(19)**:** 6156-6163.

50. Ghumman ASM NM, Shamsuddin MR, Abbasi A. Evaluation of Properties of Sulfur-based Polymers Obtained by Inverse Vulcanization: Techniques and Challenges. *Poly. & Poly. Comp.* 2021, **29** (8): 1333-1352.

51. Yan LL, Han DM, Xiao M, Ren S, Li YN, Wang SJ*, et al.* Instantaneous carbonization of an acetylenic polymer into highly conductive graphene-like carbon and its application in lithium-sulfur batteries. *J. Mater. Chem. A* 2017, **5**(15)**:** 7015-7025.

52. Shirai M, Okamura H. UV-curable positive photoresists for screen printing plate. *Polym. Int.* 2016, **65**(4)**:** 362-370.

53. Ligon-Auer SC, Schwentenwein M, Gorsche C, Stampfl J, Liska R. Toughening of photo-curable polymer networks: a review. *Polym. Chem.* 2016, **7**(2)**:** 257-286.

54.   Lengwiler G. *A History of Screen Priting: How an Art Evolved Into an Industry*. ST Media Group International, 2013.

55.   While the manuscript was under revision, a very closed DFT calculation of mechanism on vulcanization using Zinc dithiocarbamate was published, which shed light on the mechanistic study of IV reaction as well: Shi FX, Li XL, Bai YN, Li LF, Pu M, Liu L, Lei M. Mechanism of the Zinc Dithiocarbamate-Activated Rubber Vulcanization Process: A Density Functional Theory Study. *ACS Appl. Polym. Mater.* 2021, **3**, 5188-5196.

56.   Li YZ, Li Y, Liu Y, Wu YF, Wu JQ, Wang B*, et al.* Photoreduction of inorganic carbon(plus IV) by elemental sulfur: Implications for prebiotic synthesis in terrestrial hot springs. *Sci. Adv.* 2020, **6**(47): eabc3687.

57.   Frisch MJT, G.W.; Schlegel, H.B.; et al. *Gaussian 16, Revision A.03*. Gaussian Inc.: Wallingford CT, 2016.

58.   Becke AD. DENSITY-FUNCTIONAL EXCHANGE-ENERGY APPROXIMATION WITH CORRECT ASYMPTOTIC-BEHAVIOR. *Phys. Rev. A* 1988, **38**(6): 3098-3100.

59.   Perdew JP. DENSITY-FUNCTIONAL APPROXIMATION FOR THE CORRELATION-ENERGY OF THE INHOMOGENEOUS ELECTRON-GAS. *Phys. Rev. B* 1986, **33**(12): 8822-8824.

60.   Hay PJ, Wadt WR. ABINITIO EFFECTIVE CORE POTENTIALS FOR MOLECULAR CALCULATIONS - POTENTIALS FOR THE TRANSITION-METAL ATOMS SC TO HG. *J. Chem. Phys.* 1985, **82**(1): 270-283.

61.   Vosko SH, Wilk L, Nusair M. ACCURATE SPIN-DEPENDENT ELECTRON LIQUID CORRELATION ENERGIES FOR LOCAL SPIN-DENSITY CALCULATIONS - A CRITICAL ANALYSIS. *Can. J. Phys.* 1980, **58**(8): 1200-1211.

62.   Onida G, Reining L, Rubio A. Electronic excitations: density-functional versus many-body Green's-function approaches. *Rev. Mod. Phys.* 2002, **74**(2): 601-659.

63.   Zhao Y, Truhlar DG. The M06 suite of density functionals for main group thermochemistry, thermochemical kinetics, noncovalent interactions, excited states, and transition elements: two new functionals and systematic testing of four M06-class functionals and 12 other functionals. *Theor. Chem. Acc.* 2008, **120**(1-3): 215-241.